JNC TN9400 2001-005

Frequency response function method for evaluation of thermal striping phenomena

January 2000

Japan Nuclear Cycle Development Institute
O-arai Engineering Center

JNC TN9400 2001-005
January 2 0 0 0

Frequency response function method for evaluation of thermal striping phenomena

Naoto Kasahara*

Abstract

A rational analysis method of thermal stress induced by fluid temperature fluctuation is developed, by utilizing frequency response characteristics of structures. High frequency components of temperature fluctuation are attenuated in the transfer process from fluids to structures. Low frequency components hardly induce thermal stress since temperature homogenization in structures. Based on investigations of frequency response mechanism of structures to fluid temperature, a frequency response function of structures was derived, which can predict stress amplitudes on structural surfaces from fluid temperature amplitudes and frequencies. This function is formulated by separation of variables, and is composed of an effective heat transfer function and an effective thermal stress one. The frequency response function method appears to evaluate thermal stress rationally and to give information on damageable frequency range of structures.

* Structure and Material Research Group, System Engineering Division, OEC, JNC

サーマルストライピング評価のための周波数応答関数法

（研究報告書）

笠原 直人*)

要　旨

流体温度ゆらぎによる構造物の熱疲労現象はサーマルストライピングと呼ばれ、近年実プラントのき裂発生要因となったことから、日欧で評価法の開発が進められている。サーマルストライピングの従来の評価法は、温度ゆらぎデータを波形分解して温度ゆらぎ範囲と繰り返し数に変換し、これを静的に構造へ受け渡す保守的なものであった。これに対し実現象では、高周波温度ゆらぎ成分は流体から構造への伝達過程で振幅が減衰し、低周波ゆらぎは構造内熱伝導による均熱化によって熱応力に変換され難いという特性を有する。

本研究では以上の動的効果に着目し、構造の応力応答を合理的に評価する周波数応答関数を提案した。関数は熱流動現象を記述する有効熱伝達関数と、構造力学に関する有効熱応力関数との変数分離型で表される。さらに、提案した関数を設計に適用するため、汎用性を有する無次元パラメータによる設計線図を作成した。

尚、本内容は1999年9月から2000年8月までの期間にCEAカダラッシュ研究所にて実施した業務の一部である。

*) 大洗工学センター システム技術開発部 構造材料技術開発グループ

Contents

List of figures

NOMENCLATURE

$T_f(t)$: Temperature of fluid

ΔT_f : Amplitude of sinusoidal temperature fluctuation of fluid

T_{fm}: Average temperature of fluid

$T_s(x,t)$: Temperature of structure

ΔT_s : Amplitude of sinusoidal temperature fluctuation on the structural surface

$T_{s\max}$: Maximum temperature on the structural surface

$\sigma(x,t)$: Stress in structure

$\Delta\sigma|_{x=0}$: Amplitude of sinusoidal stress fluctuation on the structural surface

$\Delta\sigma_i$: Ideal stress range converted from hundred percent of fluid temperature amplitude

$G(x,t)$: Time response function of structure to fluid temperature fluctuation

$H(t)$: Time response function of effective heat transfer

$S(x,t)$: Time response function of effective thermal stress

$\phi\{T_s(x,t)\}$: Thermal stress function determined by mechanical boundary conditions

$T_f(s)$: Laplace transform of $T_f(t)$

$T_s(x,s)$: Laplace transform of $T_s(x,t)$

$G(x,s)$: Laplace transform of $G(x,t)$

$H(s)$: Laplace transform of $H(t)$

$S(x,s)$: Laplace transform of $S(x,t)$

$\Phi\{T_s(x,s)\}$: Laplace transform of $\phi\{T_s(x,t)\}$

$G(B_i, jf^*)$: Frequency response function of structural surface to fluid temperature fluctuation

$H(B_i, jf^*)$: Frequency response function of effective heat transfer

$S(jf^*)$: Frequency response function of effective thermal stress on the surface

$Bi = \dfrac{hL}{\lambda}$: Biot number

$t^* = \dfrac{ta}{L^2}$: Fourier number

$f^* = \dfrac{fL^2}{a}$: Non-dimensional frequency

x: Length from the surface of structure

t: Time

f: Frequency of sinusoidal fluctuation

h: Heat transfer coefficient

L: Wall thickness of structure

A: Area

V: Volume

a: Thermal diffusivity of structural material

λ : Heat conductivity of structural material

c: Specific heat

ρ : Density

E : *Young's* modulus of structural material

α : Linear expansion coefficient of structural material

ν : *Poisson's* ratio of structural material

K: Stress index determined by mechanical boundary conditions and material properties

$K = 1/(1-\nu)$ in the case of biaxial plane stress condition

D_f : Fatigue damage factor

N: Cycle number

N_f : Allowable cycle number of structural material

ε_t : Strain range

1 INTRODUCTION

At an incomplete mixing area of high and low temperature fluids near the structural surface, temperature fluctuation of fluid gives thermal fatigue damage on the wall structures. This coupled thermohydraulic and thermomechanical phenomenon is called thermal striping, which has so complex mechanism and sometimes causes crack initiation on the structural surfaces that sodium mock-up tests are usually required to confirm structural integrity of components. From recent needs of cost reduction, design-by-analysis methodology is strongly desired for thermal striping.

In the IAEA coordinated research program on Harmonization and validation of Fast Reactor thermomechanical and thermohydraulic codes and relations using experimental data, mechanism of thermal striping phenomenon and sensitive factors of structural integrity were investigated on a Tee junction of PHENIX secondary piping system[1]. As a result, attenuation of temperature and stress amplitude was recognized as the most important factor in the integrity assessment [2].

One of main difficulties to apply numerical approach to evaluate temperature attenuation is thermal hydraulic calculation near walls. It is required that detailed turbulent calculation methods such as DNS and LES with fine meshes less than laminar sub-layers [3], those require huge computational resources.

Another problem in mechanical side is shortage of high cycle fatigue data to evaluate large number of strain cycles caused from high frequency fluctuation.

In order to overcome above difficulties, author paid attention to following structural characteristics. Wall structures can not respond to high frequency fluctuation of fluid temperature because of heat transfer loss [4][5] and low frequency components of fluctuation may not cause large thermal stresses since thermal homogenization in materials [6] as in Fig.1. These tendencies are easily understood from F.E. calculations of a plate wall subjected to sinusoidal temperature fluctuation of fluid. Fig.2 is temperature history on the inner and outer surfaces, and Fig.3 is stress one on the both surfaces. By utilizing these characteristics, we can limit damageable frequencies to structural materials that have to be evaluated. In order to quantify frequency response characteristics, author has proposed the structural response diagram, where stress amplitude of structures can be predicted against the temperature fluctuation with a constant frequency and a heat convection factor [7].

This theoretical study will propose ideas to extend the concept of structural response diagram and develop general frequency response function.

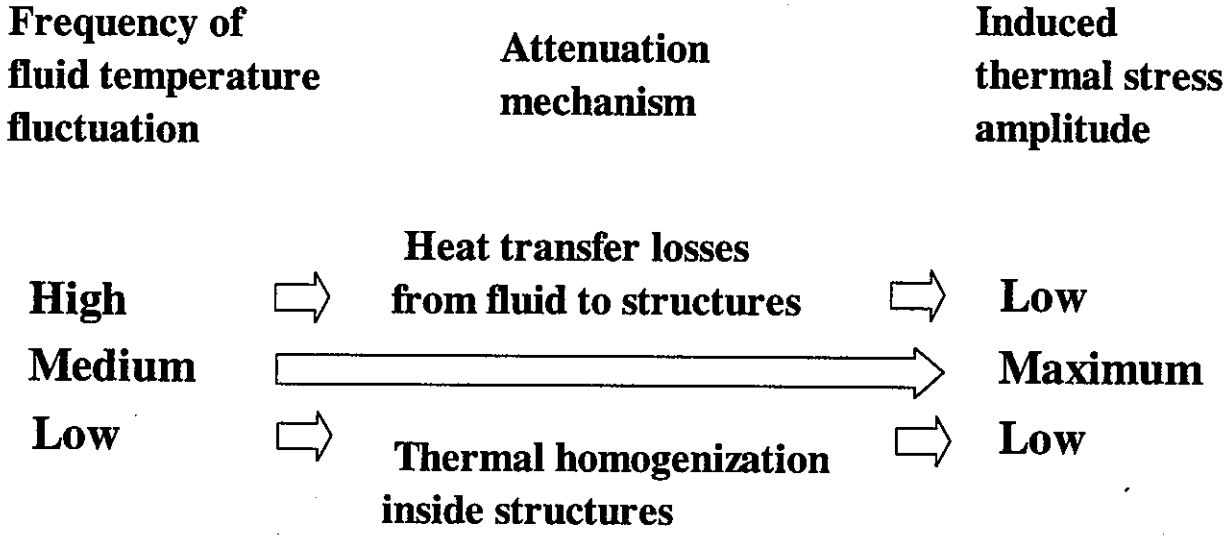

Fig.1 General tendency of structural response to fluid temperature fluctuation

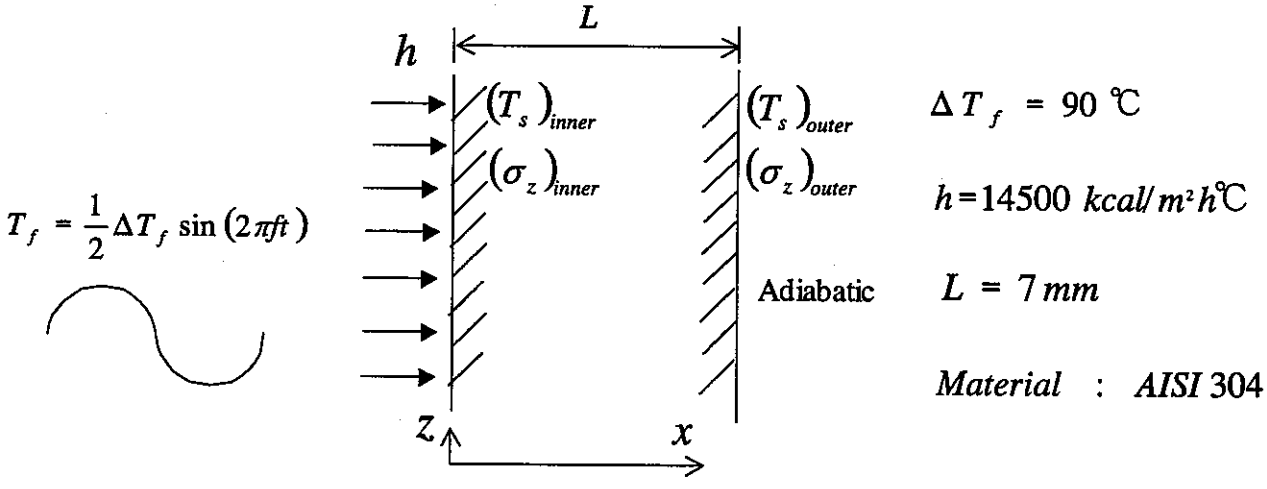

Fig.2 Wall model with boundary conditions for F.E. calculations

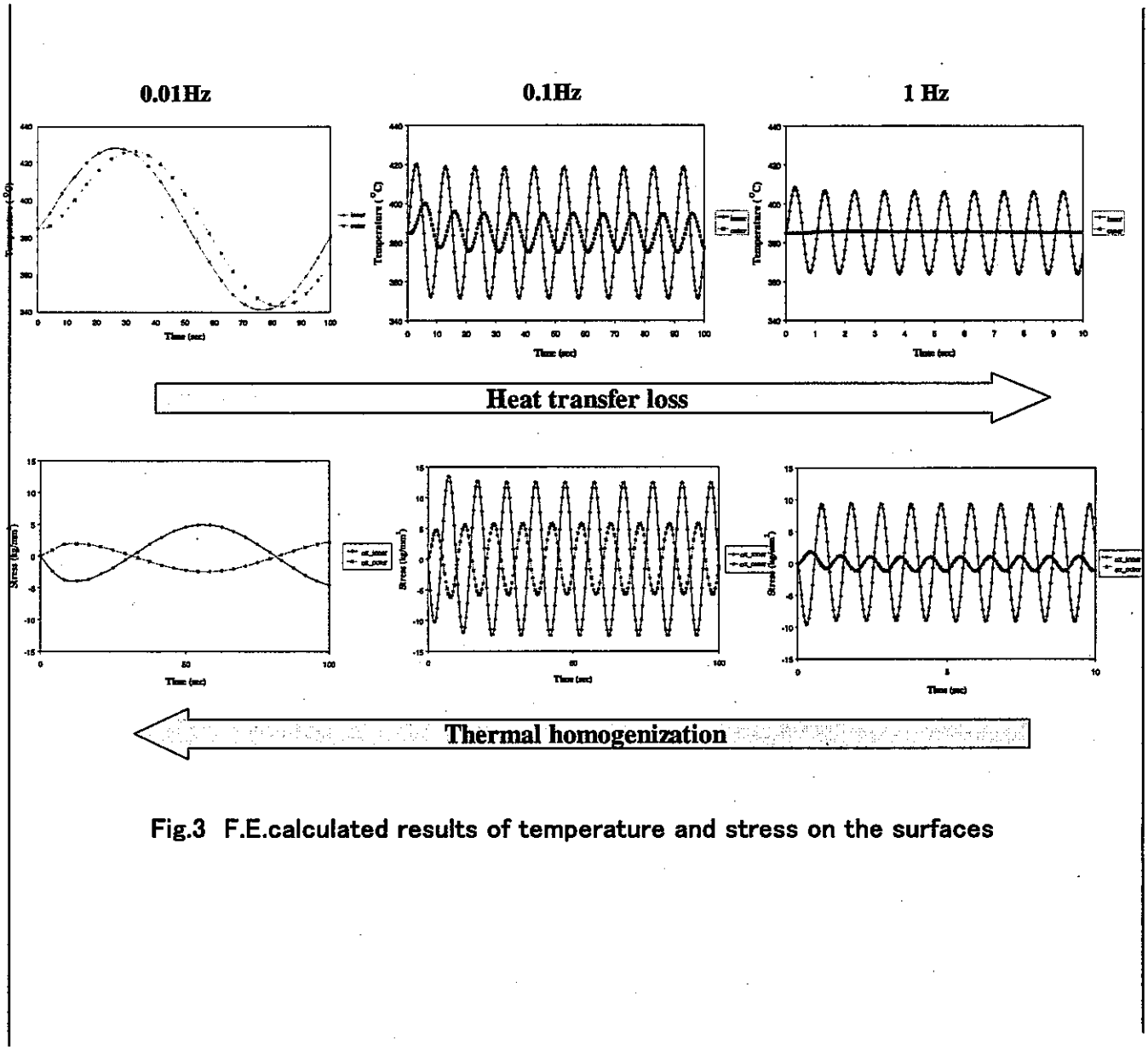

Fig.3 F.E.calculated results of temperature and stress on the surfaces

2. FORMULATION OF PHENOMENA BY FREQUENCY TRANSFER FUNCTIONS

2.1. ONE DEGREE OF HEAT CAPACITY PROBLEM

In order to understand mechanism of structural responses to fluid temperature fluctuations, thermal and mechanical responses problems are theoretically formulated. Fig.4 is a one degree of heat capacity model as the most simple problem. Its differential equation with a boundary condition is

$$Vc\rho\dot{T}_s + AhT_s = AhT_f \tag{1}$$

$$T_f = \frac{1}{2}\Delta T_f \sin(\omega t). \tag{2}$$

Laplace transform of Eq.(1) is

$$(Vc\rho s + Ah)T_s(s) = AhT_f(s). \tag{3}$$

Transfer function H(s) from fluid temperature $T_f(s)$ to structural temperature $T_s(s)$ can be described as

$$H(s) = \frac{T_s(s)}{T_f(s)} = \frac{1}{1+\tau s}, \quad \tau = \frac{Vc\rho}{Ah}. \tag{4}$$

Frequency response function is

$$H(j\omega) = \frac{1}{1+j\omega\tau} \tag{5}$$

Such frequency dependent characteristics is explained from Eq.(5), that $\omega \to \infty$, $|H(j\omega)| \to 0$.

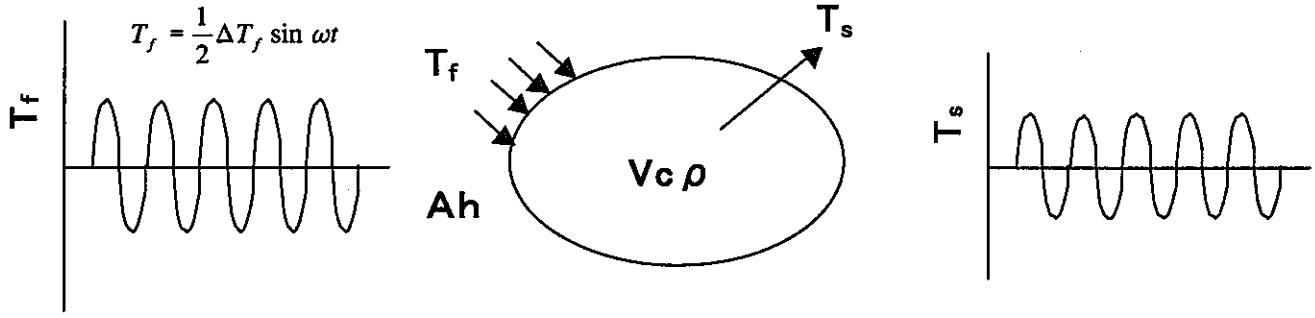

Fig.4 One degree of heat capacity problem

2.2. TWO DEGREES OF HEAT CAPACITY PROBLEM

Next problem described in Fig.5 is a two degrees of heat capacity model. In this problem, thermal stress is assumed to be proportional to difference between two heat capacity points as

$$\sigma = KE\alpha(T_{s0} - T_{s1}), \tag{6}$$

where K is a stress factor determined from a geometry.

Differential equation with boundary condition is

$$\begin{bmatrix} V_0 c_0 \rho_0 & 0 \\ 0 & V_1 c_1 \rho_1 \end{bmatrix} \begin{Bmatrix} \dot{T}_{s0} \\ \dot{T}_{s1} \end{Bmatrix} + \begin{bmatrix} A_0 h + A_1 \lambda_1 & -\frac{A_1 \lambda_1}{L_1} \\ -\frac{A_1 \lambda_1}{L_1} & \frac{A_1 \lambda_1}{L_1} \end{bmatrix} \begin{Bmatrix} T_0 \\ T_1 \end{Bmatrix} = \begin{bmatrix} A_0 h & 0 \\ 0 & 0 \end{bmatrix} \begin{Bmatrix} T_f \\ 0 \end{Bmatrix}, \tag{7}$$

where A_0 is a convection area, A_1 is conductive area, L_1 is conductive length with heat conductivity λ_1.

Transfer function from fluid temperature to stress can be obtained by Laplace transform of Eqs.(6) and (7) as

$$\frac{\sigma(s)}{T_f(s)} = \frac{T_{s0}(s)}{T_f(s)} \cdot \frac{\sigma(s)}{T_{s0}(s)} = \cdot KE\alpha H(s) S(s) = KE\alpha G(s). \tag{8}$$

In Eq.(8), H(s) is an effective heat transfer function described as

$$H(s)=\frac{T_{s0}(s)}{T_f(s)}=\frac{1}{1+\tau_f s},\quad \tau_f=\frac{V_0 c_0 \rho_0}{A_0 h}. \tag{9}$$

which is the same as Eq.(5), and

S(s) is an effective thermal stress function expressed as

$$S(s)=\frac{1}{KE\alpha}\frac{\sigma(s)}{T_{s0}(s)}=1-\frac{1}{1+\tau_s s},\quad \tau_s=\frac{V_1 c_1 \rho_1 L_1}{A_1 \lambda_1}. \tag{10}$$

Frequency response function of two degrees of heat capacity is obtained from Eq.(8) as

$$G(j\omega)=KE\alpha\frac{1}{1+j\omega\tau_f}\cdot\frac{j\omega\tau_s}{1+j\omega\tau_s} \tag{11}$$

From Eq.(11), it is obtained that $\omega\to 0,\ |G(j\omega)|\to 0$ and $\omega\to\infty,\ |G(j\omega)|\to 0$.

Consequently, general tendency of frequency response shown in Fig.1 can be explained by two degrees of heat capacity model.

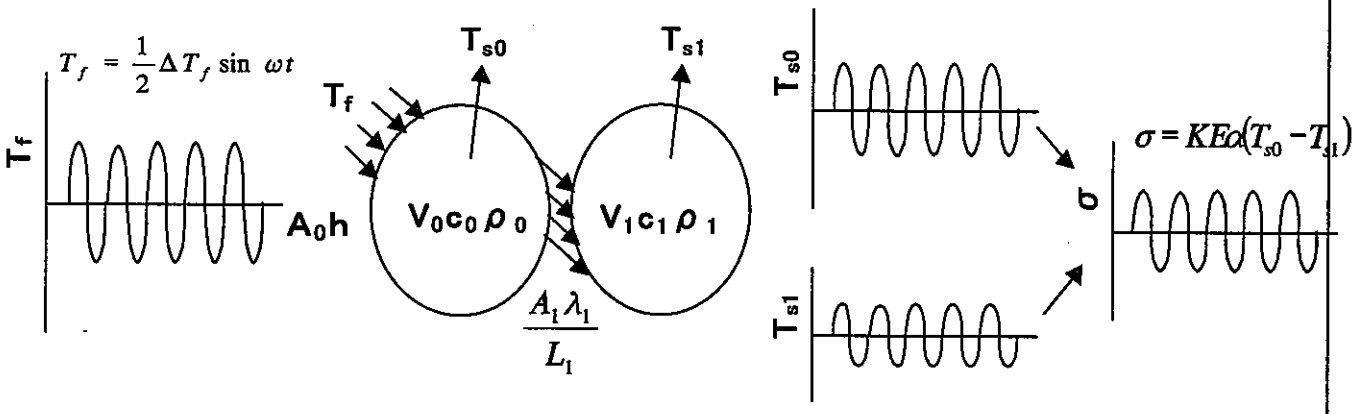

Fig.5 Two degrees of heat capacity problem

2.3. CONTINUUM HEAT CONDUCTION PROBLEM

The third problem is a continuum heat conduction model as in Fig.6, where thermal stress is assumed to be described with a mechanical equation which depends on mechanical boundary conditions as

$$\sigma(x,t) = KE\alpha\phi\{T_s(x,t)\}. \tag{12}$$

Here, $\phi\{T_s(x,t)\}$ becomes zero when $T_s(x,t)$ is constant except a full constraint condition.

Partial differential equation of heat conduction is

$$c\rho\frac{\partial T_s}{\partial t} + \lambda\frac{\partial^2 T_s}{\partial x^2} = 0. \tag{13}$$

General expression of thermal boundary conditions are

$$aT_s(0,t) + b\frac{\partial}{\partial x}T_s(0,t) = A(T_f) \tag{14}$$

$$cT_s(L,t) + d\frac{\partial}{\partial x}T_s(L,t) = B(t). \tag{15}$$

Transfer function from fluid temperature to thermal stress can be described as

$$\frac{\sigma(x,s)}{T_f(s)} = \frac{T_s(0,s)}{T_f(s)}\cdot\frac{T_s(x,s)}{T_s(0,s)}\cdot\frac{\sigma(x,s)}{T_s(x,s)} = KE\alpha H(s)S(x,s) = KE\alpha G(x,s). \tag{16}$$

In Eq.(16), H(s) is an effective heat transfer function described as

$$H(s) = \frac{T_s(0,s)}{T_f(s)} \tag{17}$$

which was introduced from Eq.(13) with thermal boundary conditions Eqs.(14)(15).
And S(x,s) is an effective thermal stress function expressed as

$$S(x,s)=\frac{1}{KE\alpha}\cdot\frac{T_s(x,s)}{T_s(0,s)}\cdot\frac{\sigma(x,s)}{T_s(x,s)}=\frac{T_s(x,s)}{T_s(0,s)}\cdot\Phi(T_s(x,s)) \tag{18}$$

which depends on the thermal equation Eq.(13) with boundary conditions Eq.(15) and the mechanical one Eq.(12).

Since Eqs.(16)(17)(18) are general expressions, an example solution is calculated for the case of a=1, b=-1 and $A(T_f)=T_f$ in Eq.(14) and d=0 and B(t)=0 in Eq.(15) as,

$$H(s)=\frac{-1}{s\left(\sqrt{s}\coth\sqrt{s}+1\right)} \tag{19}$$

$$S(x,s)=\frac{\sinh\left\{(1-x/L)\sqrt{s}\right\}}{\sinh\sqrt{s}}\Phi(T_s(x,s)) \tag{20}$$

Frequency response function obtained from Eq.(16) with Eqs(19)(20) is

$$\frac{\sigma(x,j\omega)}{T_f(j\omega)}=KE\alpha G(x,j\omega)=KE\alpha H(j\omega)S(x,j\omega) \tag{21}$$

When H(s) is described by Eq.(19), $\omega\to\infty$ leads to $|G|\to 0$.

When S(x,s) is described by Eq.(20), $\omega\to 0$ leads to $|G|\to 0$ since temperature homogenization makes $\Phi(T_s(x,s))$ zero.

Eq.(21) is more general expression than Eq.(11). Thus, frequency response characteristics of structures can be formulated by separation of variables composed of an effective heat transfer function H jω) and an effective thermal stress S(jω).

Detailed transfer functions for various boundary conditions will be studied in the later sections.

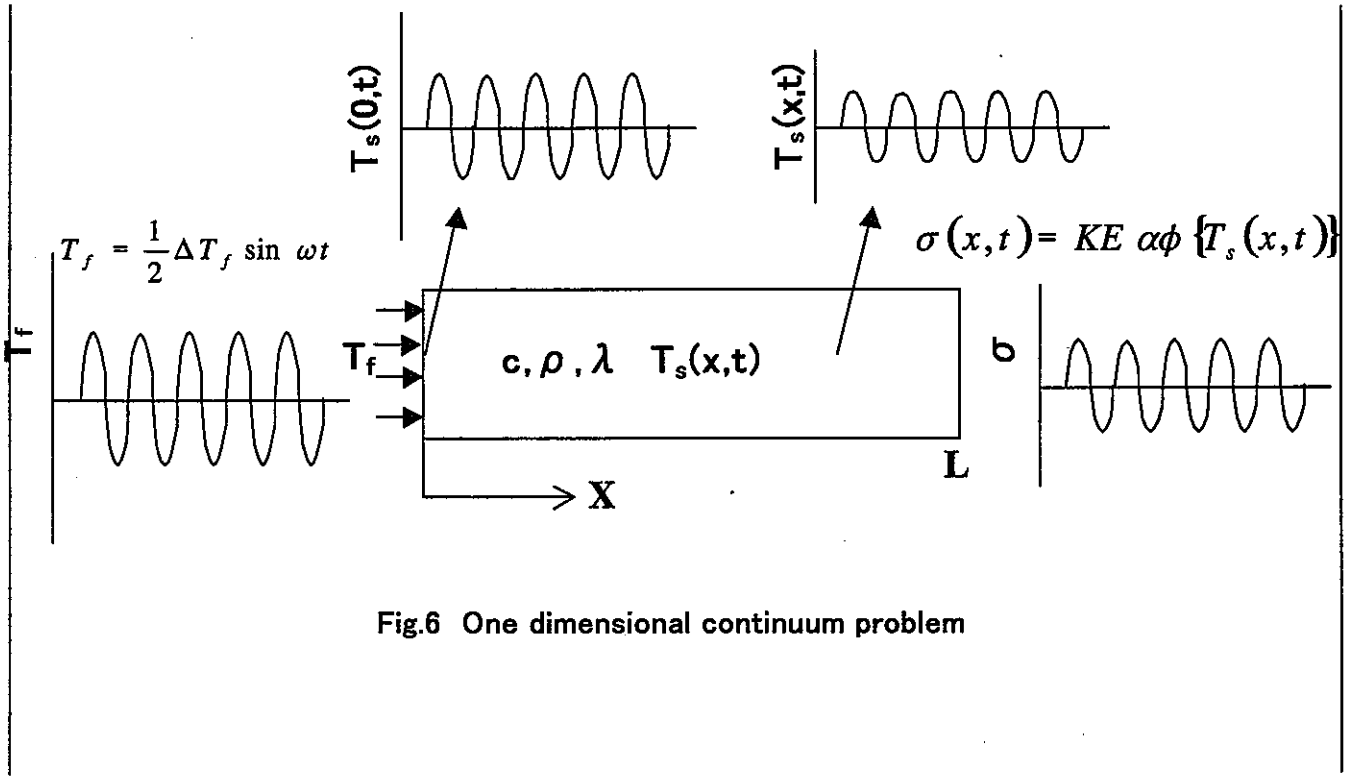

Fig.6 One dimensional continuum problem

3. EFFECTIVE HEAT TRANSFER FUNCTION

3.1. MECHANISM OF HEAT TRANSFER LOSS

It was observed from experimental study on thermal response of structures to fluid temperature fluctuation, that temperature amplitude attenuated during transfer process from fluids to structures when frequencies become high [4]. On the other hand, an amplitude was less attenuated when flow rates increase under a constant zero-cross frequency [5].

Detailed mechanisms of heat transfer loss were investigated through sodium experiments and their analyses [9]. As the results, factors of temperature attenuation was understood as (1) convection mixing, (2) turbulent mixing, and (3) molecular diffusion as in Fig.7.

Since actual heat transfer process of thermal striping is non-stationary, time average turbulent models such as K-ε are not applicable. It is required that detailed turbulent analysis methods such as Direct Navier-Stokes Simulation (DNS) and Large Eddy Simulation (LES).

Existence of thermal interaction between fluids and structures may affect these phenomena. Thermal coupling between fluids and structures can be considered by a heat conduction model without introduction of heat transfer coefficients. Here, wall functions are difficult to be adopted because heat fluxes on the structural surfaces are sensitive to local temperature distributions near the walls. Sufficient fine grid models are required to evaluate non-linear temperature gradients inside Laminar sub-layers (Conductive Layers). Simulations with above methods consume so huge computation resources, that techniques such as local grid refinement are necessary to realize long physical time simulation that is enough to evaluate low frequency components of fluctuation.

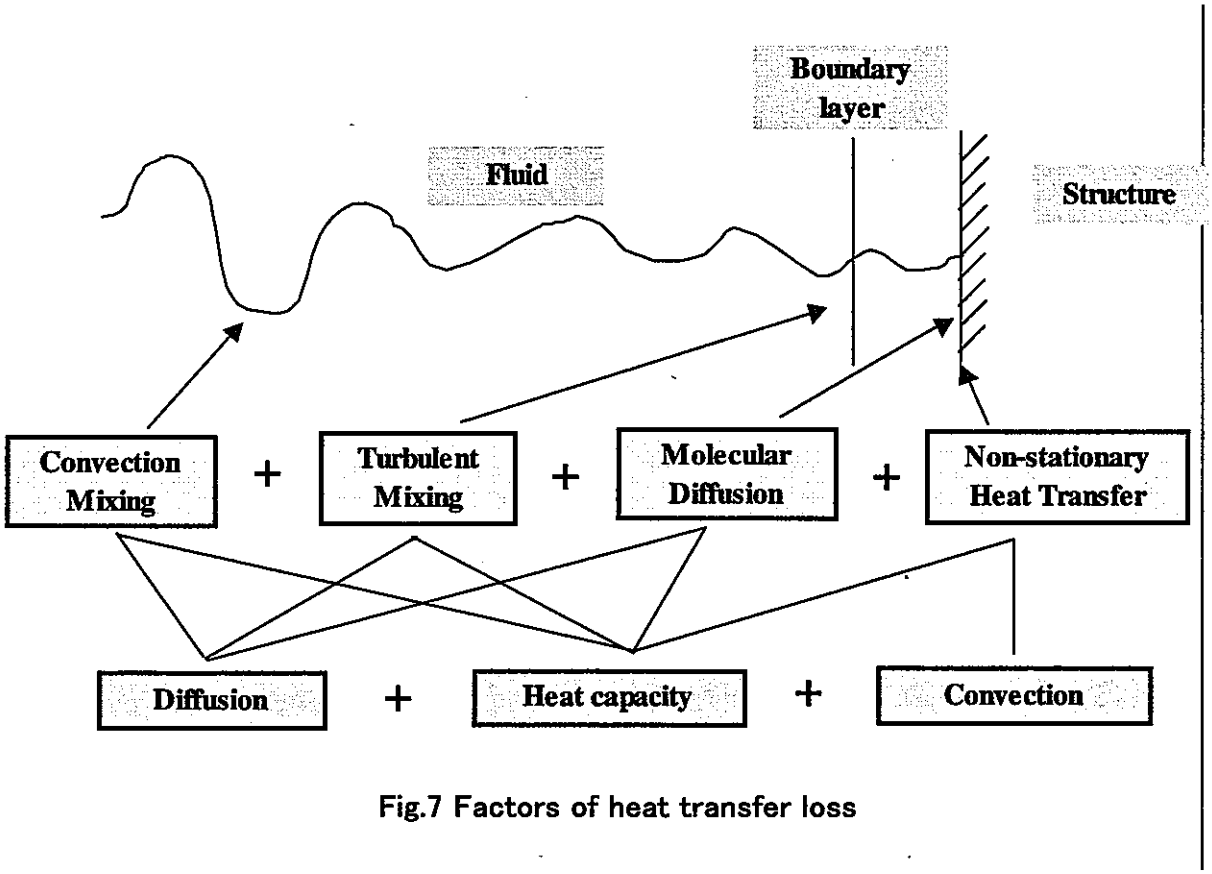

Fig.7 Factors of heat transfer loss

When phenomena are considered as stationary, heat transfer coefficients defined between steady state main flows and structures become to be applicable.

Since damageable frequencies are usually so low from frequency response characteristics of structures that they seem to be considered as semi-stationary phenomena.

To investigate applicability of equivalent heat transfer coefficient, non-stationary numerical simulations are planned in the EJCC framework for observing time histories of heat fluxes on the structural surfaces with temperature differences between structural surfaces and fluid near walls.

In this paper, sensitivities of heat transfer loss to frequencies are roughly investigated as preliminary study. Attenuation factors described in Fig.7 are composed of such fundamental phenomena as (a) response delay from heat capacity, (b) thermal diffusion, and (c) loss of heat convection.

Frequency characteristics of the simplest models corresponding to above fundamental phenomena are as follows:

(a) Heat capacity

Time response of a heat capacity model described in Fig.8(a) is

$$T_s = \frac{a}{\sqrt{1+(\omega\tau)^2}}\sin(\omega t + \phi) - \frac{a\sin\phi}{\sqrt{1+(\omega\tau)^2}}e^{-t/\tau} \quad \tau = \frac{Vc\rho}{Ah}. \tag{22}$$

Frequency response characteristics of Eq.(22) is

$$|H(j\omega)| = \frac{1}{\sqrt{1+(\omega\tau)^2}} \tag{23}$$

$$\angle H(j\omega) = -\tan^{-1}\omega\tau \tag{24}$$

By introducing normalized frequency $\omega^* = \tau\omega$, Eq.(23) can be reduced to be

$$|H(j\omega^*)| = \frac{1}{\sqrt{1+(\omega^*)^2}} \tag{25}$$

(b) Diffusion

Time response of a 1D diffusion model [10] shown in Fig.8(b) is

$$T_s = Ae^{-kx}\sin(\omega t - kx), \quad k = \sqrt{\frac{\omega}{2a}}, \quad a = \frac{\lambda}{c\rho}. \tag{26}$$

Frequency response characteristics of Eq.(26) is

$$|H(j\omega)| = e^{-kx} \tag{27}$$

$$\angle H(j\omega) = -kx \tag{28}$$

By introducing normalized frequency $\omega^* = \frac{\omega}{2a}$, gain of Eq.(27) can be reduced to be

$$|H(j\omega^*)| = e^{-\sqrt{\omega^*}x} \tag{29}$$

(c) Convection

Time response of a 1D convection model [10] described in Fig.8(c) is

$$T_s(x,t) = \frac{Ah^*}{\sqrt{(h^*+k)^2+k^2}} e^{-kx} \sin(\omega t - kx - \varepsilon)$$

$$\varepsilon = \tan^{-1}[k/(h^*+k)],\ h^* = \frac{h}{\lambda} \tag{30}$$

Frequency response characteristics on the surface is obtained from Eq.(30) as

$$H(j\omega) = \frac{T_s(0,j\omega)}{T_f(j\omega)} \tag{31}$$

$$|H(j\omega)| = \frac{h^*}{\sqrt{(h^*+k)^2+k^2}} \tag{32}$$

$$\angle H(j\omega) = -\tan^{-1}[k/(h^*+k)] \tag{33}$$

By introducing normalized frequency $\omega^* = \frac{\omega}{2a}$, gain of Eq.(32) can be reduced to be

$$|H(j\omega^*)| = \frac{h^*}{\sqrt{(h^*+\sqrt{\omega^*})^2+\omega^*}} \tag{34}$$

Sensitivities of gains to frequency are compared among capacity, diffusion, and convection. Gain $|H(j\omega^*)|$ calculated by Eqs(25),(29),(34) under assumption of x=1 and h*=1 are compared as in Fig.9. These results suggest that all of fundamental phenomena have the similar tendency of frequency characteristics and capacity and diffusion exhibit stronger attenuation than convection in the high frequency regime. As the result, there is the possibility that heat transfer function considering heat convection can approximate heat transfer loss conservatively.

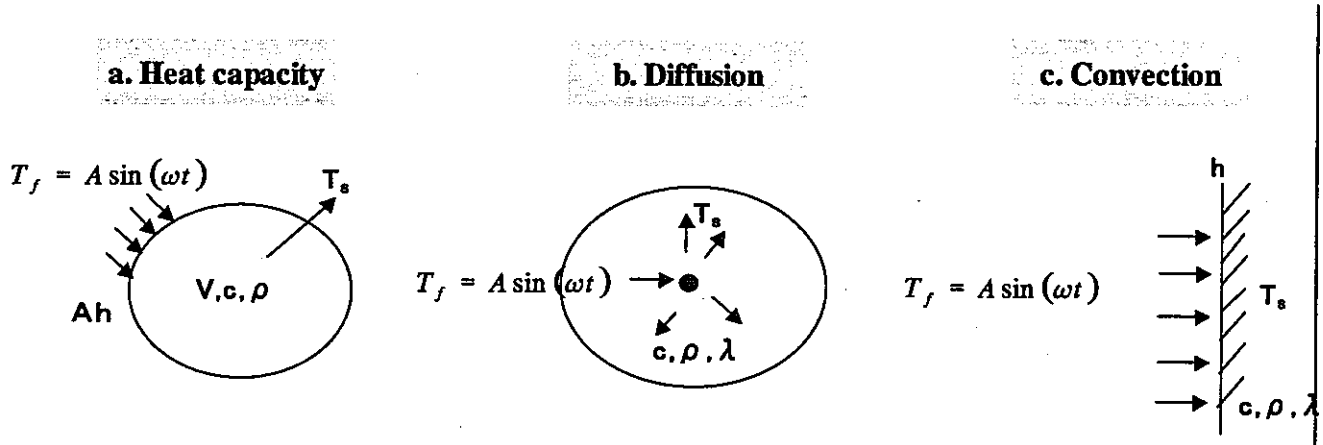

Fig.8 Frequency characteristics models of fundamental phenomena

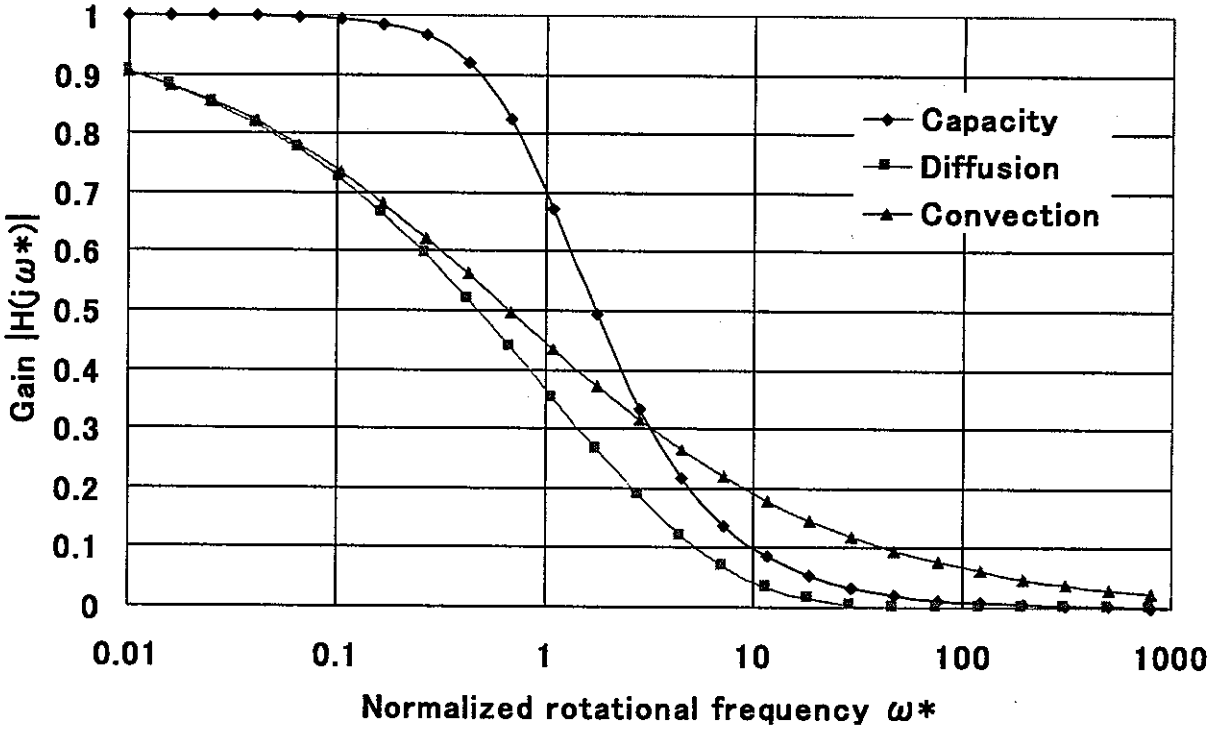

Fig.9 Frequency characteristics of heat transfer models

3.2. APPROXIMATION BY HEAT TRANSFER FUNCTION

Effective heat transfer function is introduced under assumption of a heat convection model.

Since boundary conditions of the back surface have few effects to temperature on the surface due to temperature fluctuation except for very thin structures and for very low frequencies, a semi-infinite model such as Fig.8(c) is assumed to evaluate surface temperature. Thermal stress of very thin structures and stress caused from very low frequency fluctuation are generally so small from thermal homogenization, that this assumption comes into existence for practical use.

From this model, Eqs.(32) (33) of frequency response functions were introduced. In order to make more general expression, representative length L (wall thickness for example) is introduced as in Fig.10

By multiplying L to both of numerators and denominators, Eqs.(32) (33) can be reduced to be functions of non-dimensional parameters $Bi = \frac{hL}{\lambda}$ and $f^* = \frac{fL^2}{a}$

as

$$|H(j\omega)| = \frac{\frac{h}{\lambda}}{\sqrt{\left(\frac{h}{\lambda}+\sqrt{\frac{\omega}{2a}}\right)^2+\left(\sqrt{\frac{\omega}{2a}}\right)^2}} = \frac{L\frac{h}{\lambda}}{\sqrt{\left(L\frac{h}{\lambda}+\sqrt{L^2\frac{\omega}{2a}}\right)^2+\left(\sqrt{L^2\frac{\omega}{2a}}\right)^2}} = \frac{B_i}{\sqrt{\left(B_i+\sqrt{\pi f^*}\right)^2+\pi f^*}} \tag{35}$$

$$\angle H(j\omega) = -\tan^{-1}\frac{\sqrt{\frac{\omega}{2a}}}{\frac{h}{\lambda}+\sqrt{\frac{\omega}{2a}}} = -\tan^{-1}\frac{\sqrt{L^2\frac{\omega}{2a}}}{L\frac{h}{\lambda}+\sqrt{L^2\frac{\omega}{2a}}} = -\tan^{-1}\frac{\sqrt{\pi f^*}}{B_i+\sqrt{\pi f^*}} \tag{36}$$

Gain of effective heat transfer function can be described as

$$\left|\mathrm{H}(B_i, jf^*)\right| = \frac{B_i}{\sqrt{\left(B_i+\sqrt{\pi f^*}\right)^2+\pi f^*}} \tag{37}$$

diagram of which is shown as in Fig.11

Phase delay of effective heat transfer function can be described as

$$\angle H(B_i, j\omega) = -\tan^{-1}\frac{\sqrt{\pi f^*}}{B_i+\sqrt{\pi f^*}} \tag{38}$$

diagram of which is shown as in Fig.12.

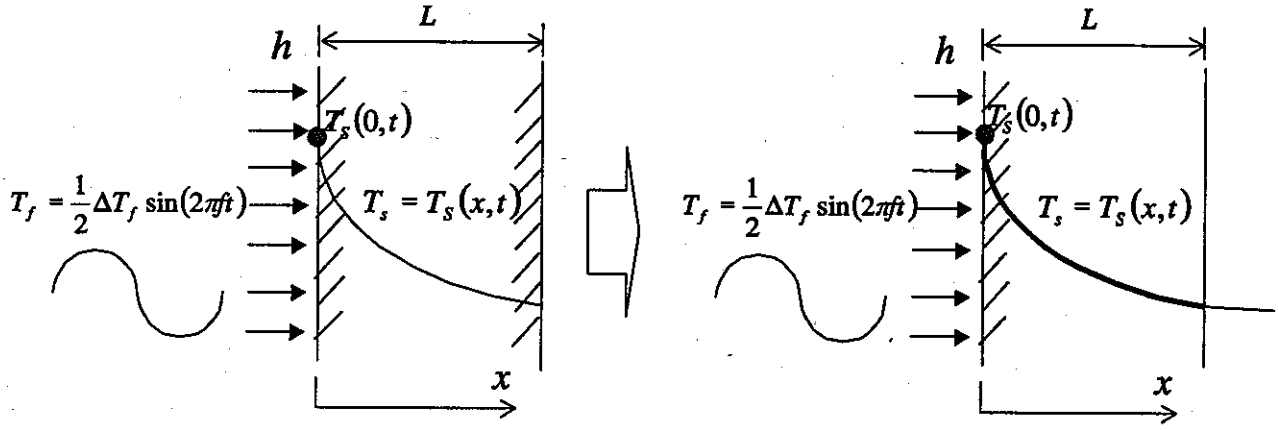

Fig.10 Thermal response model of a semi-infinite solid to sinusoidal temperature fluctuation of fluid

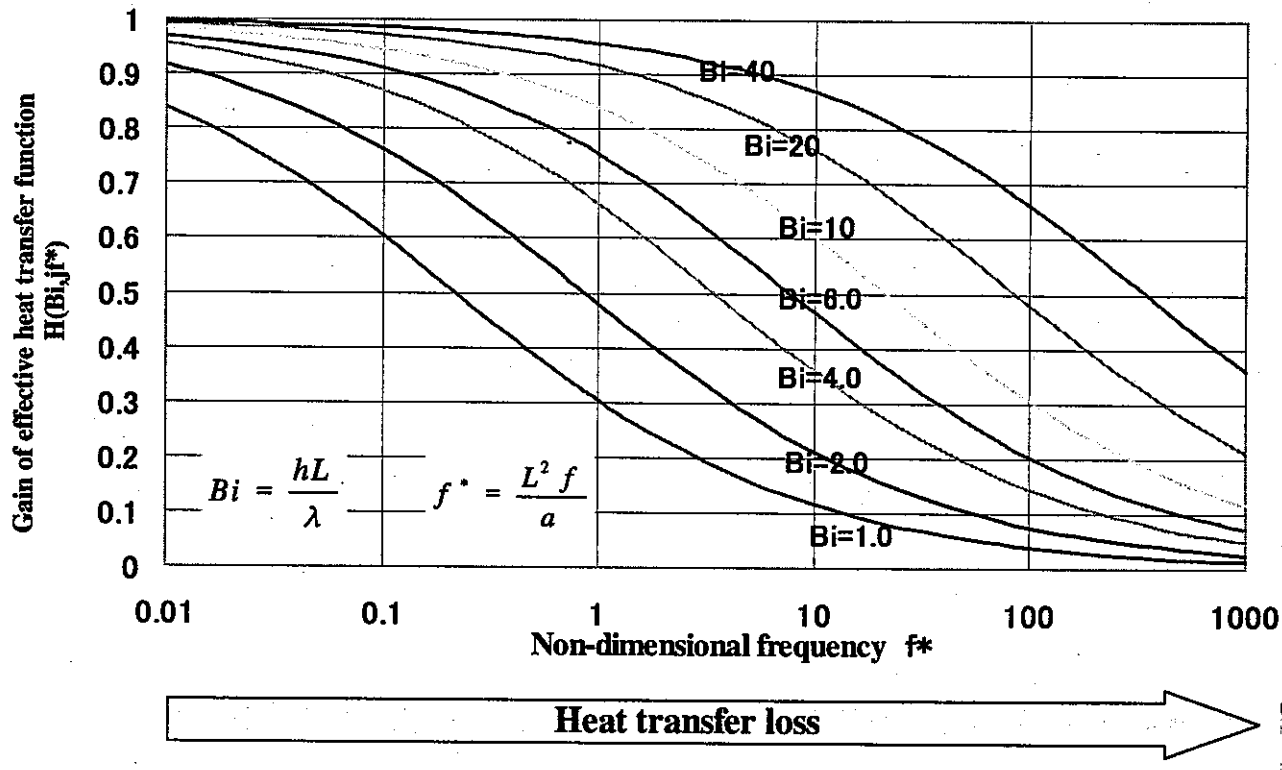

Fig.11 Gain of effective heat transfer function

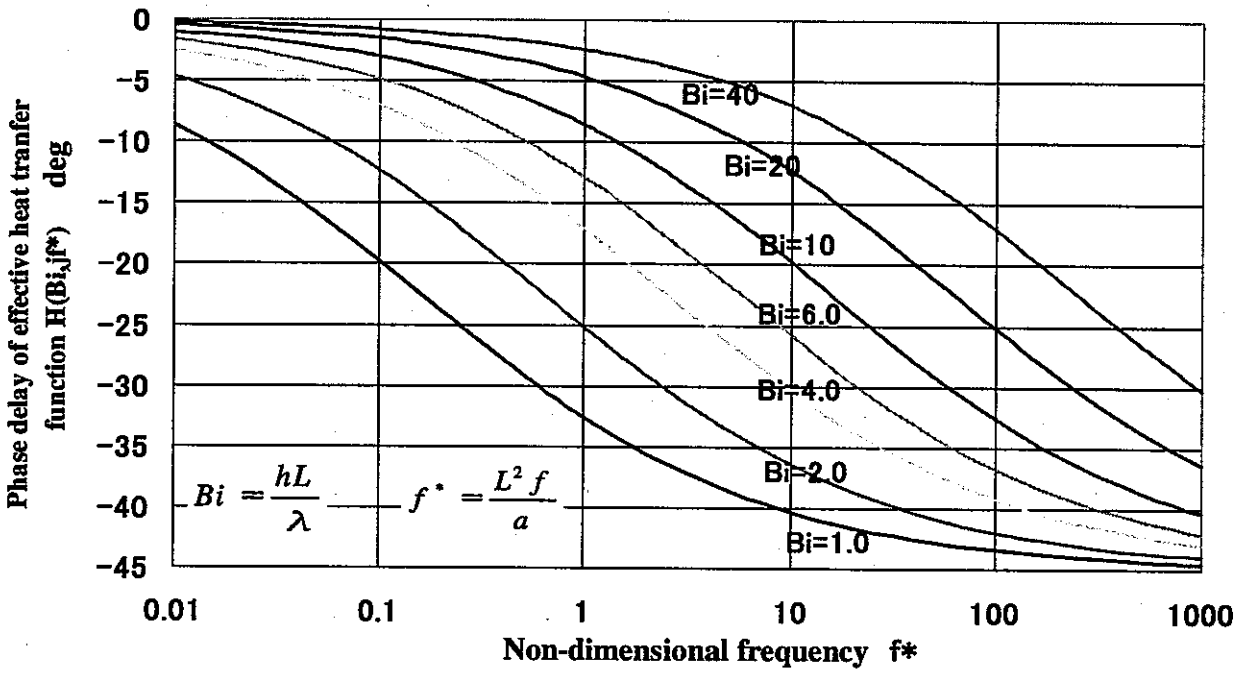

Fig.12 Phase delay of effective heat transfer function

4. EFFECTIVE THERMAL STRESS FUNCTION

4.1. THERMAL STRESS FUNCTION UNDER VARIOUS CONSTRAINT CONDITIONS

Effective thermal stress function described by Eq.(19) means a transfer function from temperature fluctuations on the structural surfaces to induced thermal stress. Since thermal stress is affected by temperature distribution in structures and constraint conditions, effective thermal stress S(x,s) depends on both thermal and mechanical boundary conditions. This function was studied under various boundary conditions in literature[11].

In actual components of plants, outer surfaces of structural walls can be assumed adiabatic compared with fluid sides, so that thermal boundary condition is described by c=0 and B(t)=0 in Eq.(15). Under this thermal boundary condition, effective thermal stress functions on the surface $s(0, jf^*) = s(jf^*)$ can be introduced as functions of $f^* = \frac{fL^2}{a}$ for three kinds of constraint conditions (Fig.13), from the literature [11].

(a) Constraint free

$$s(jf^*) = -(B + jC) + (B_m + jC_m) + (B_b + jC_b) \tag{39}$$

(b) Bending constraint

$$s(jf^*) = -(B + jC) + (B_m + jC_m) \tag{40}$$

(c) Membrane plus bending constraint

$$s(jf^*) = -(B + jC) \tag{41}$$

Where,

$$B = \frac{PR + QS}{R^2 + S^2}, \quad C = \frac{QR - PS}{R^2 + S^2}$$

$$P = R = \cos\sqrt{\pi f^*}\cosh\sqrt{\pi f^*}, \quad Q = S = \sin\sqrt{\pi f^*}\sinh\sqrt{\pi f^*}$$

$$B_m = \frac{1}{2\sqrt{\pi f^*}}\left[\frac{\sin\sqrt{\pi f^*}\cos\sqrt{\pi f^*} + \sinh\sqrt{\pi f^*}\cosh\sqrt{\pi f^*}}{\cos^2\sqrt{\pi f^*}\cosh^2\sqrt{\pi f^*} + \sin^2\sqrt{\pi f^*}\sinh^2\sqrt{\pi f^*}}\right]$$

$$C_m = \frac{1}{2\sqrt{\pi f^*}}\left[\frac{\sin\sqrt{\pi f^*}\cos\sqrt{\pi f^*} - \sinh\sqrt{\pi f^*}\cosh\sqrt{\pi f^*}}{\cos^2\sqrt{\pi f^*}\cosh^2\sqrt{\pi f^*} + \sin^2\sqrt{\pi f^*}\sinh^2\sqrt{\pi f^*}}\right]$$

$$B_b = \frac{3}{2\sqrt{\pi f^*}}\left[\frac{\sinh\sqrt{\pi f^*}\cosh\sqrt{\pi f^*} + \sin\sqrt{\pi f^*}\cos\sqrt{\pi f^*} - \dfrac{2\sinh\sqrt{\pi f^*}\sin\sqrt{\pi f^*}}{\sqrt{\pi f^*}}}{\cos^2\sqrt{\pi f^*}\cosh^2\sqrt{\pi f^*} + \sin^2\sqrt{\pi f^*}\sinh^2\sqrt{\pi f^*}}\right]$$

$$C_b = \frac{3}{2\sqrt{\pi f^*}}\left[\frac{\begin{array}{l}-\sinh\sqrt{\pi f^*}\cosh\sqrt{\pi f^*} + \sin\sqrt{\pi f^*}\cos\sqrt{\pi f^*} \\ + \dfrac{2}{\sqrt{\pi f^*}}\left(\cos^2\sqrt{\pi f^*}\cosh^2\sqrt{\pi f^*} + \sin^2\sqrt{\pi f^*}\sinh^2\sqrt{\pi f^*} - \cosh\sqrt{\pi f^*}\cos\sqrt{\pi f^*}\right)\end{array}}{\cos^2\sqrt{\pi f^*}\cosh^2\sqrt{\pi f^*} + \sin^2\sqrt{\pi f^*}\sinh^2\sqrt{\pi f^*}}\right]$$

Gain of effective thermal stress functions

$$\left|S(jf^*)\right| = \sqrt{\mathrm{Re}^2 + \mathrm{Im}^2} \qquad (42)$$

for three kinds of constraint conditions were calculated as in Fig.14 , where Re is real part of Eqs.(39)(40)(41) and Im is imaginative part of them.

It is understood from these results that gain of effective thermal stress functions become large when strongly constrained.

Phase delay of effective thermal stress functions

$$\angle S(jf^*) = -\tan^{-1}\frac{\mathrm{Im}}{\mathrm{Re}} \qquad (43)$$

for three kinds of constraint conditions were calculated as in Fig.15.

Constraint conditions are affected by three-dimensional temperature distribution such as hot spot, wall thickness, and multi axial stress condition. Therefore, actual constraint conditions are intermediate among above three conditions. Typical structures of FBR components are considered as bending constraint. In the case of very thin shell structures such as thermal liners, constraint is free.

Membrane plus constraint conditions should be avoided in design stage.
However, there is possibility that it appeasers when hot/cold spots are enforced to thick wall structures.

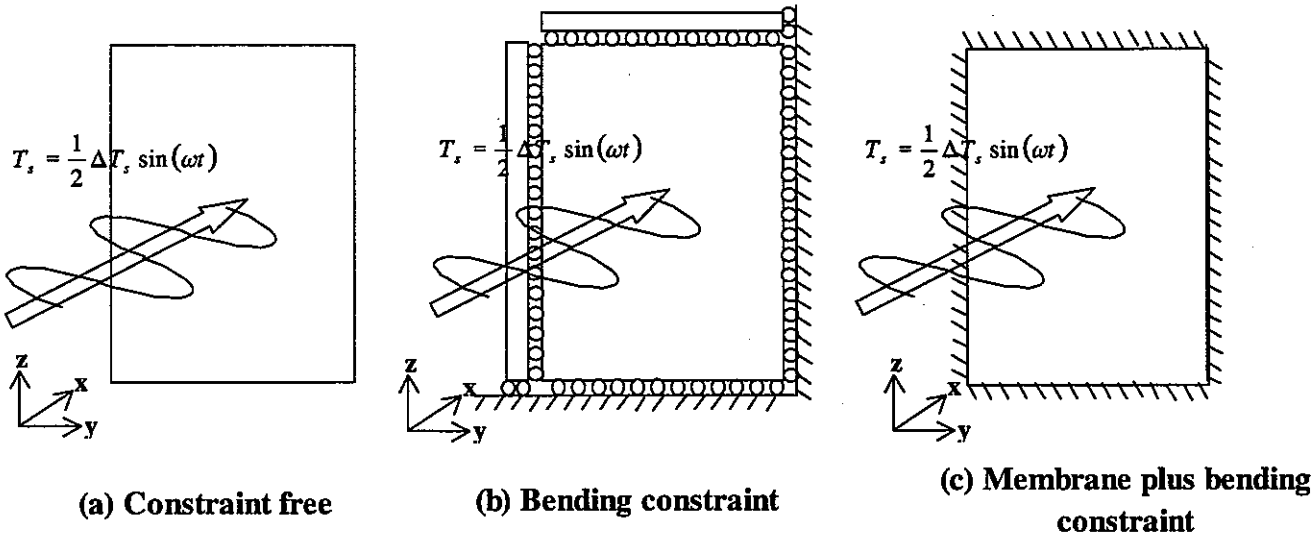

(a) Constraint free

(b) Bending constraint

(c) Membrane plus bending constraint

Fig.13 Variations of constraint conditions

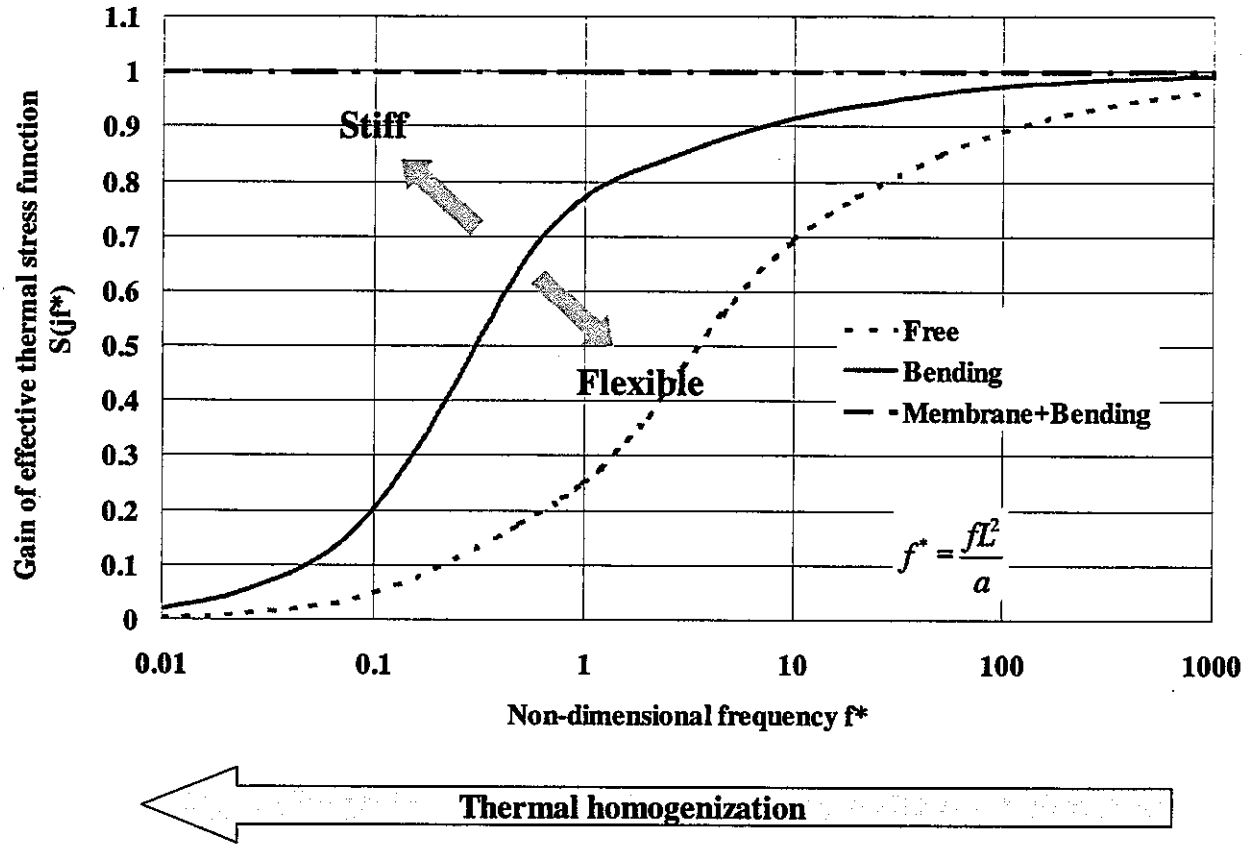

Fig.14 Gain of effective thermal stress function

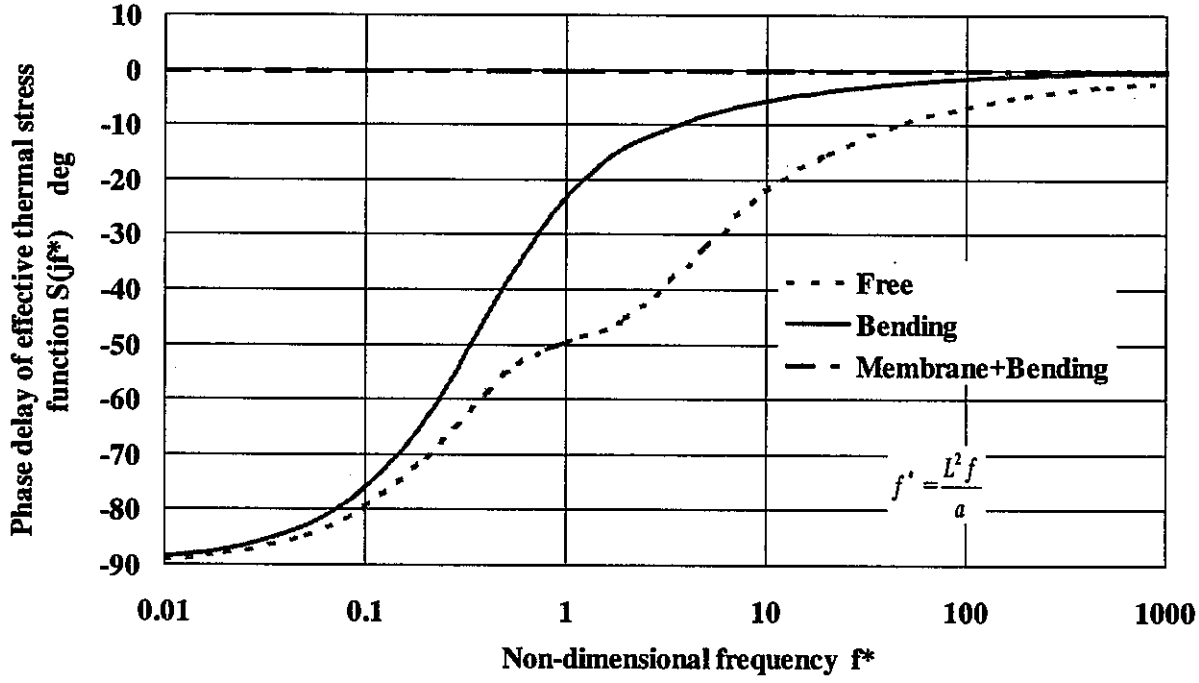

Fig.15 Phase delay of effective thermal stress function

4.2. FREQUENCY RESPONSE FUNCTION WITH EFFECTIVE HEAT TRANSFER FUNCTION

By substituting $H(B_i, jf^*)$ and $S(jf^*)$ to Eq.(21), frequency transfer function from fluid temperature to thermal stress is described as

$$G(B_i, jf^*) = H(B_i, jf^*)S(jf^*). \tag{44}$$

Gain of frequency transfer function

$$|G(B_i, jf^*)| = |H(B_i, jf^*)||S(jf^*)| \tag{45}$$

under bending constraint condition can be obtained from Eqs.(37)(40)(42) as in Fig.16 of diagram.

By using this diagram, induced stress range can be easily evaluated from temperature range of fluid as

$$\Delta\sigma|_{x=0} = KE\alpha\Delta T_f|G(B_i, jf^*)| . \tag{46}$$

Phase delay of frequency transfer function

$$\angle G(B_i, jf^*) = \angle H(B_i, jf^*) + \angle S(jf^*) \tag{47}$$

is also evaluated from Eqs.(38)(40)(42) as in Fig.17 of diagram.

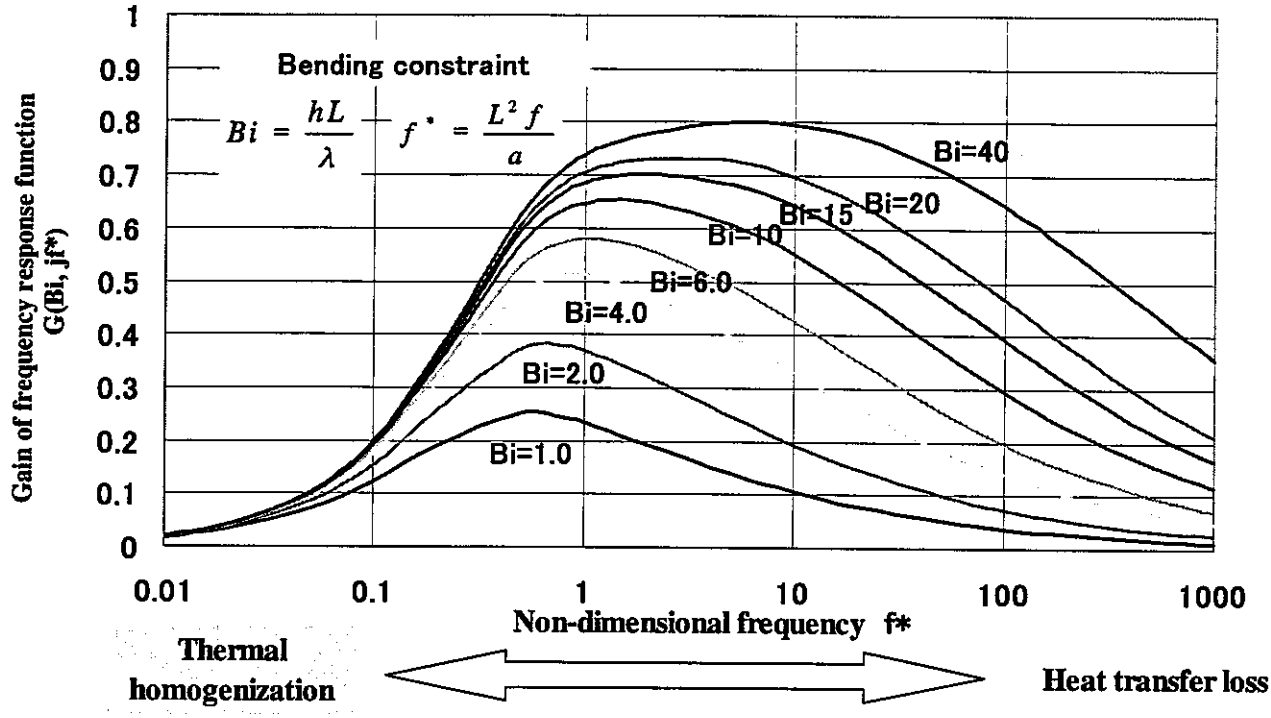

Fig.16 Gain of frequency stress response to fluid temperature fluctuation
(Bending constraint condition)

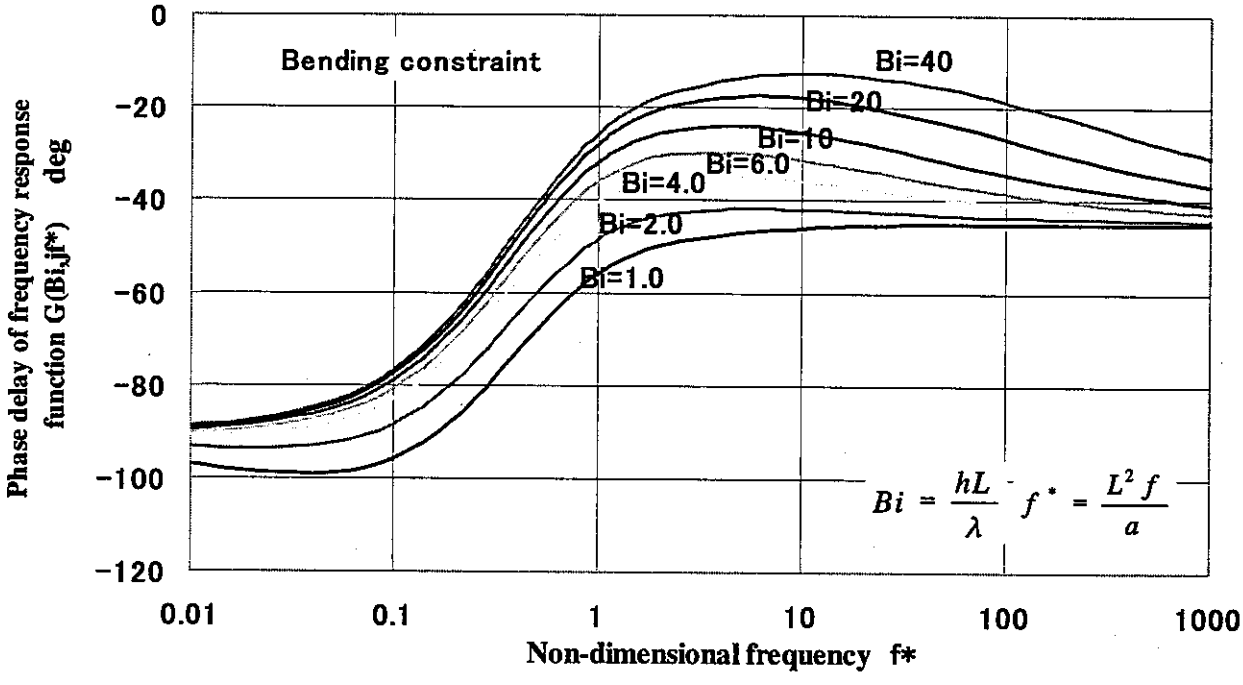

Fig.17 Phase delay of frequency stress response to fluid temperature fluctuation
(Bending constraint condition)

By substituting Eqs.(37)(38)(39)(42)(43) to Eq.(21), diagram of frequency transfer function from fluid temperature to thermal stress under constraint free condition can be obtained. Gain of the function is as in Fig.18 and phase delay of one is shown in Fig.19.

When substituting Eqs.(37)(38)(41)(42)(43) to Eq.(21), diagram of frequency transfer function from fluid temperature to thermal stress under membrane plus bending constraint condition can be obtained. Gain of the function is as in Fig.20 and phase delay of one is shown in Fig.21.

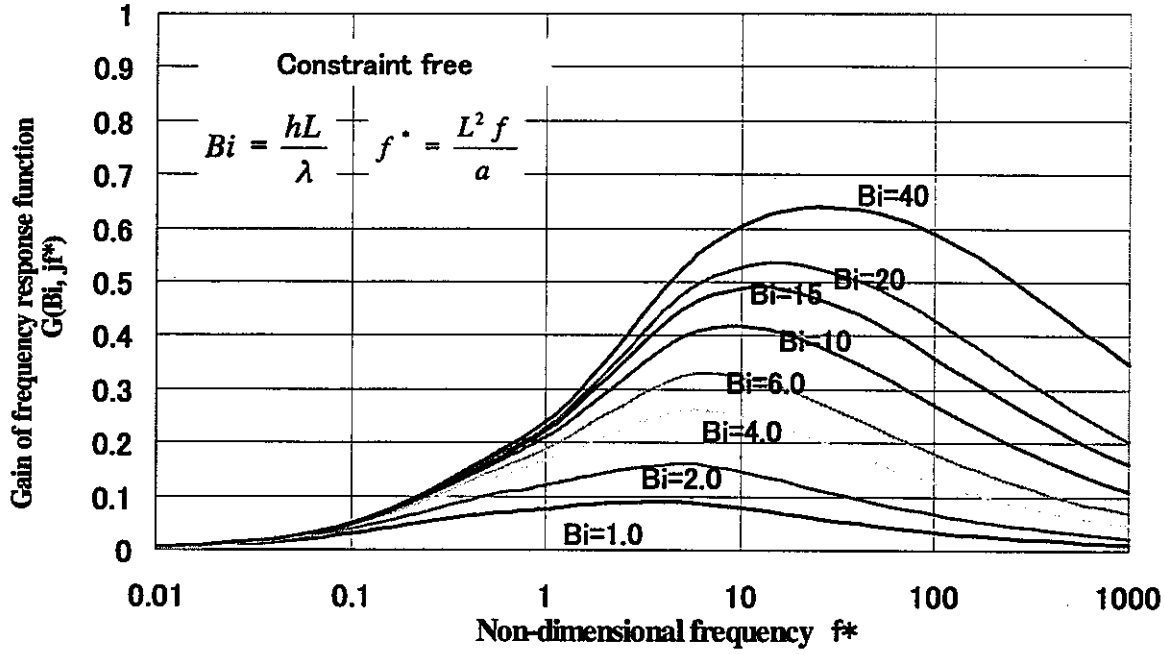

Fig.18 Gain of frequency stress response to fluid temperature fluctuation
(Constraint free condition)

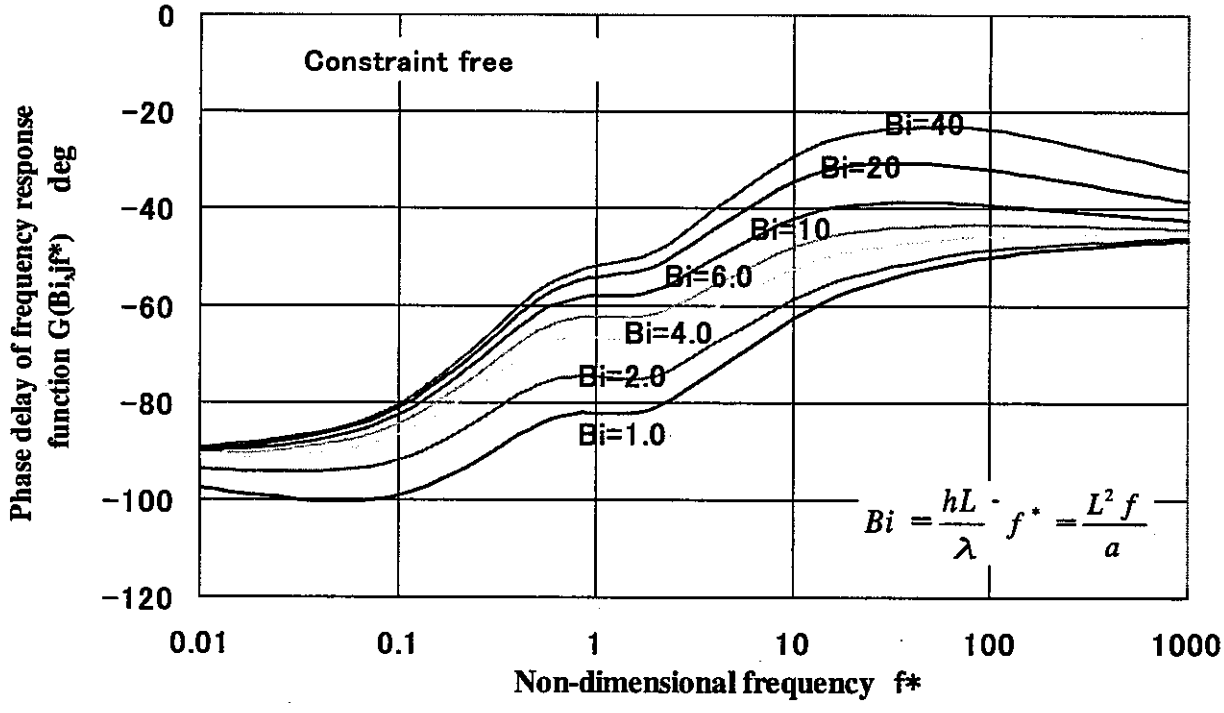

Fig.19 Phase delay of frequency stress response to fluid temperature fluctuation
(Constraint free condition)

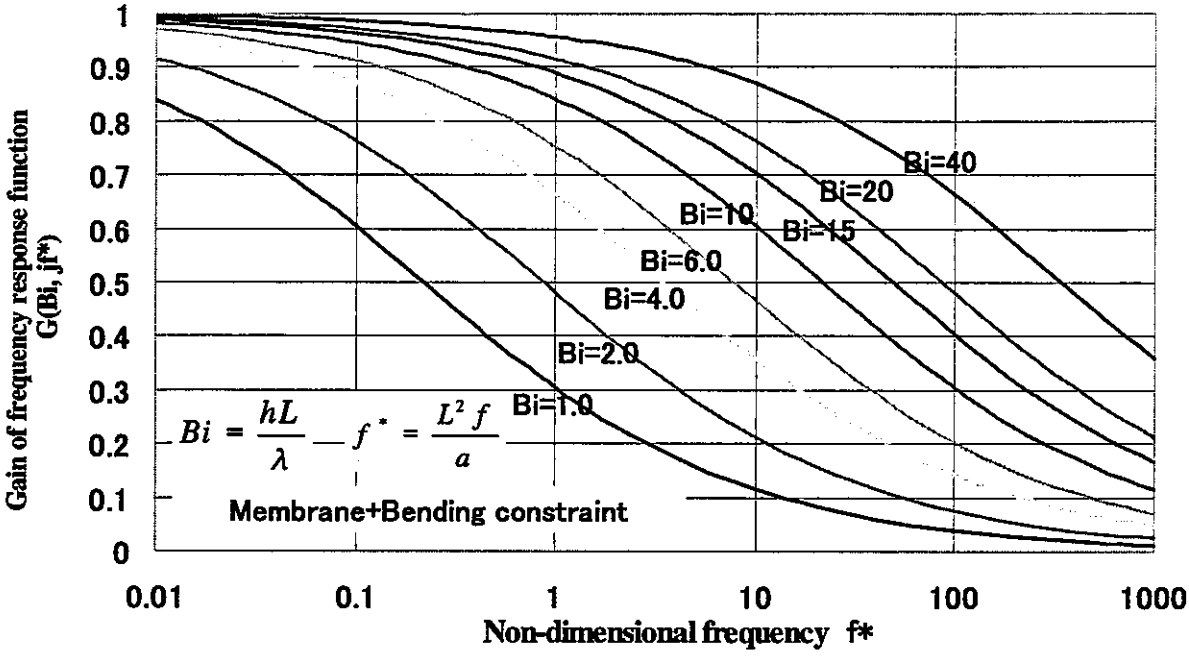

Fig.20 Gain of frequency stress response to fluid temperature fluctuation
(Membrane plus bending constraint condition)

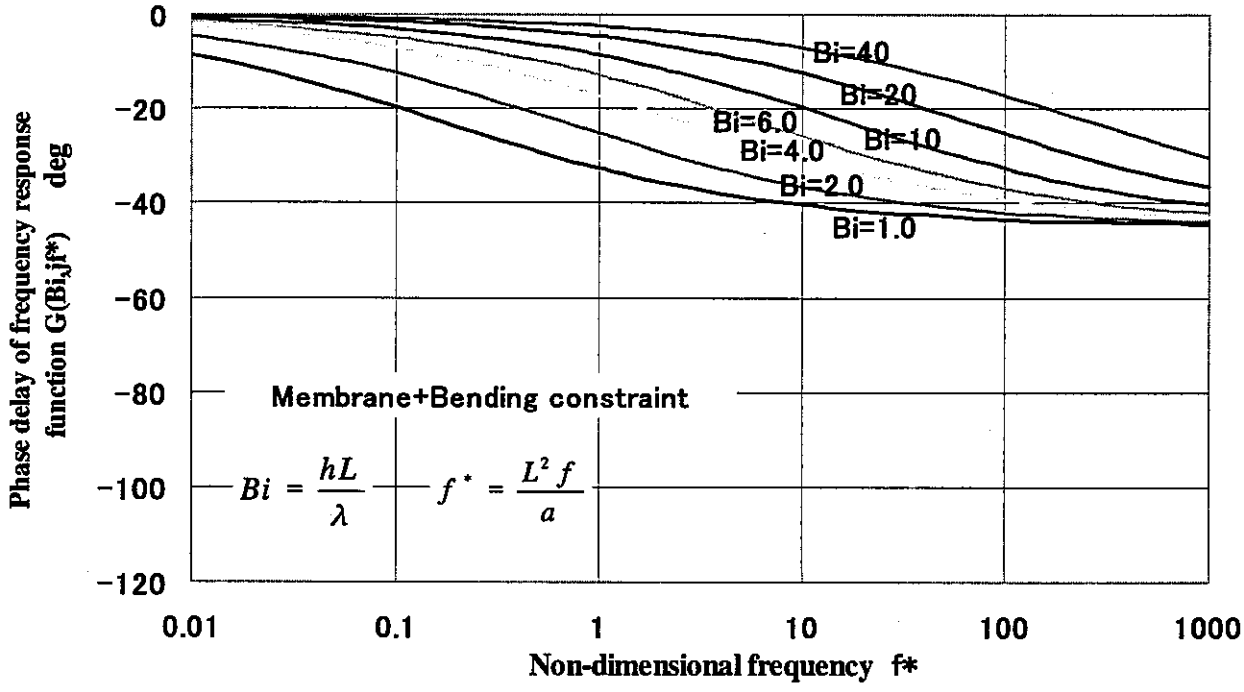

Fig.21 Phase delay of frequency stress response to fluid temperature fluctuation
(Membrane plus bending constraint condition)

5. FATIGUE STRENGTH ANALYSIS WITH A FREQUENCY TRANSFER FUNCTION

When introducing service period, frequencies can be converted into cycle numbers and it enables direct comparison of frequency response diagrams with fatigue curves of materials. For example, gain diagrams of frequency response functions under assumption of 30 years operation period and 100℃ fluid temperature amplitude were compared with fatigue curves of stainless steels as in Fig.22. Here, strain ranges were calculated from stress ranges of frequency response diagrams under assumption of elastic deformation. Parameters of frequency response diagrams are wall thickness and heat transfer coefficients. Such fatigue curves were over plotted that extrapolated curves from low cycle fatigue data of 316FR under are three kinds of frequencies (JNC 316FR), French high cycle fatigue data (RCC-MR) and Japanese high cycle data (JNC 304).

Fatigue damage factor Df for each cycle can be evaluated by using Fig.22 and *Miner's* rule,

$$D_f = \sum \frac{N(\varepsilon_t)}{N_f(\varepsilon_t)} \tag{48}$$

and results in the case of JNC 316FR 0.1Hz are in Fig.23. This figure explains that fatigue damage is sensitive to narrow band of frequency and fatigue data over 10^9 cycles is not necessary for fatigue analysis.

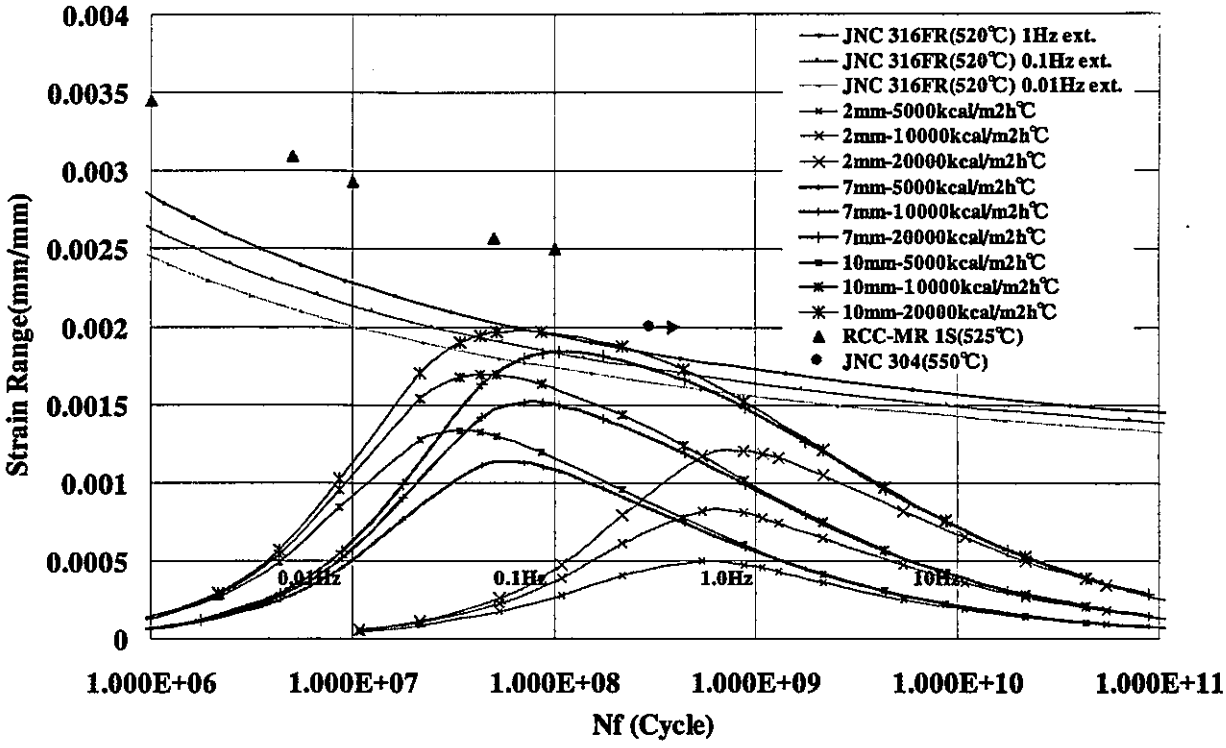

Fig.22 Comparison between fatigue curves and frequency response diagrams (30years, ΔT_f=100℃)

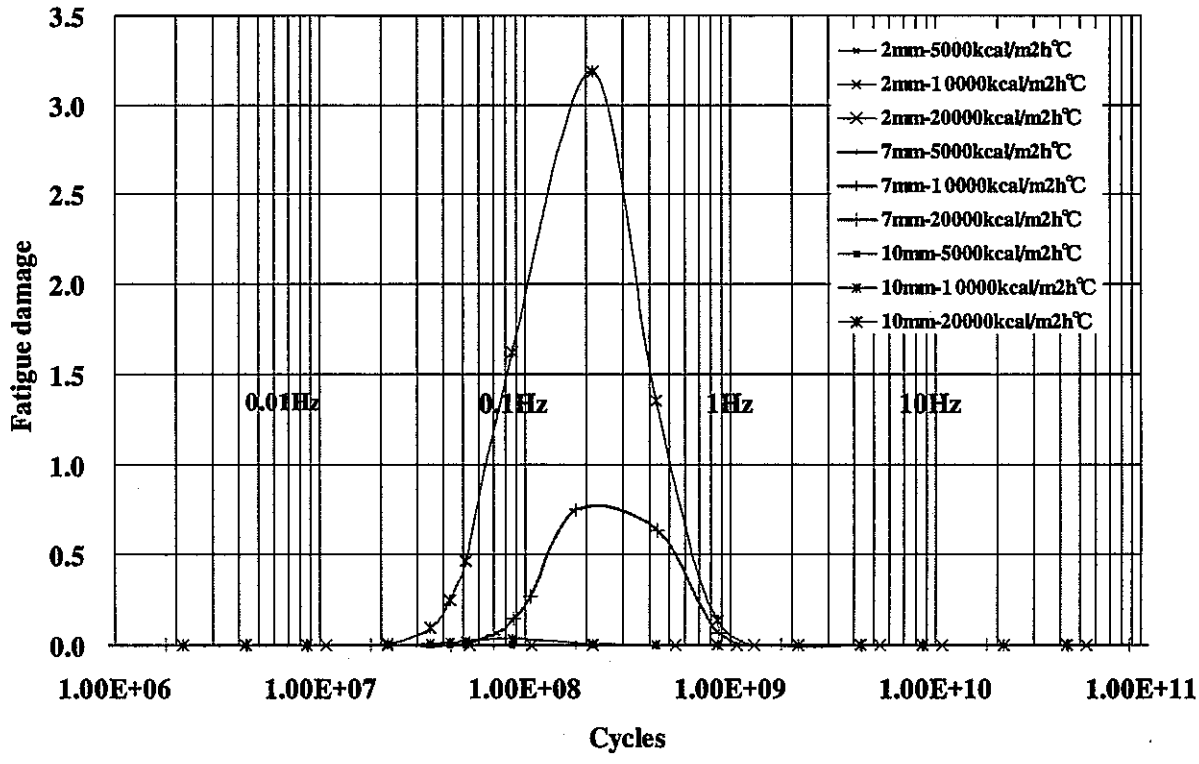

Fig.23 Calculated fatigue damage (30years, ΔT_f=100℃, 316FR,0.1Hz)

6. CONCLUSIONS

Structural response mechanism to fluid temperature fluctuation was clarified and was formulated by the frequency response function. This function is described by separation of variables, which composed, of an effective heat transfer function and an effective thermal stress one. The effective heat transfer function can describe that high frequency components of temperature fluctuation are attenuated from heat transfer loss. The effective thermal stress function can explain that low frequency components of fluctuation hardly induce thermal stress because of thermal homogenization.

Multiplication of both functions indicates damageable frequency range to structures. Thermal stress induced by sinusoidal temperature fluctuation can be rapidly evaluated by this function. Finally fatigue strength analysis method with the frequency response function was proposed.

7. DISCUSSIONS

The effective heat transfer function is based on a heat convection model. It is necessary to examine applicability of a heat convection model and to develop an evaluation method of equivalent heat convection coefficients.

The effective thermal stress function depends on constraint conditions. When constraint conditions will be identified, this approach can be applied to general structures including hot and cold spots. A guideline to evaluate constraint conditions in actual components is desirable.

Validation of proposed methods by temperature and thermal fatigue strength data of FAENA [12] and TIFFSS [13] is planned.

In order to evaluate actual thermal striping phenomena, this method will be extended to random fluctuations. To examine its applicability, fatigue analysis results based on frequency response functions will be compared with results by other methods such as Rain-flow and Zero-cross wave counting techniques. Furthermore, introduction of statistical approach may be necessary to extrapolate results from short period data to long life evaluation of actual components.

ACKNOWLEDGEMENT

It is very thankful in discussion and guiding from Dr.Y. Lejeail of CEA-Cadarache on FAENA experiments. Several helpful discussions in thermal hydraulic field with Dr. T.Muramatsu, Mr. H.Kamide, and Mr. M.Nishimura of OEC/JNC, Dr. P.Roubin of CEA-Cadarache, and Dr. J.P.Simoneau of Framatome are gratefully acknowledged. Thanks are due to Ms. O. Gelineau of Framatome who gave suggestion on sinusoidal approach. The author is also deeply indebted to Dr. C.Poette and Dr. M.T. Cabrillat of CEA-Cadarache and Dr.M.Morishita of OEC/JNC for their kindness to make a chance of cooperative work under the EJCC contract

REFERENCES

[1] Muramatsu,T., Evaluation of Thermal Striping Phenomena at a Tee Junction of LMFR Piping System with Numerical Methods (1) Thermohydraulic Calculations, SMiRT15, F05/6, (1999)

[2] Kasahara,N., Evaluation of Thermal Striping Phenomena at a Tee Junction of LMFR Piping System with Numerical Methods (2) Thermomechanical Calculations, SMiRT15, F05/5, (1999)

[3] Muramatsu,T., Experimental and Numerical Results on Non-Stationary Thermal Response Characteristics for a Fluid-Structure Interaction System, E-J Thermal-Hydraulics Specialist Meeting, CEA France,(1998)

[4] Buffet.J.C. and Tenchine,D., Transfer of temperature fluctuations across boundary layers in turbulent liquid metal flows, ASME,PVP Vol.98 pp153/157(1985)

[5] Wakamatsu,M., Attenuation of temperature fluctuations in thermal striping, J.Nucl.Sci.Technol., Vol.32,No.8,pp38/48(1995)

[6] Boley, B.A., Theory of Thermal Stresses, John Wiley & Sons,(1960)

[7] Kasahara,N. et al., Structural Response Diagram Approach for Evaluation of Thermal Striping Phenomenon, SMiRT15, F05/4,(1999)

[8] Farlow,S.J., Partial differential equations for scientists and engineers, John Wiley & Sons,(1982)

[9] Muramatsu,T., Numerical Analysis of Non - Stationary Thermal Response Characteristics for a Fluid - Structure Interaction System, ASME,PVP377,(1998)

[10] Holman, J.P,Heat Transfer, 7th ed., McGraw-Hill, (1990)

[11] Jones,I., The effect of various constraint conditions in the frequency response model of thermal striping, Fatigue Fract.Engng Mater.Struct. Vol.18, No.4, pp489/502,(1995)

[12] Astegiano, J.C. and Lejeail, Y., Overview of thermal fatigue tests performed on FAENA sodium loop, February 5, (1999)

[13] Kasahara,N. and Lejeail, Y., Benchmark problems on thermal striping evaluation of FAENA and TIFFSS sodium experiments, JNC TN9400 2001-006,(2000)